T-count optimization of approximate quantum Fourier transform

Byeongyong Park[1, 2], Doyeol (David) Ahn[1, 2, 3]*

[1]*Department of Electrical and Computer Engineering and Center for Quantum Information Processing, University of Seoul, 163 Seoulsiripdae-ro, Dongdaemun-gu, Seoul 02504, Republic of Korea*

[2]*First Quantum Inc., 2F-210, Sparkplus, 180, Bangbae-ro, Seocho-gu, Seoul 06586, Republic of Korea*

[3]*Physics Department, Charles E. Schmidt College of Science, Florida Atlantic University, 777 Glades Road, Boca Raton, FL 33431-0991, USA*

*Corresponding author: dahn@uos.ac.kr

Abstract: The quantum Fourier transform (QFT) is a ubiquitous quantum operation that is used in numerous quantum computing applications. The major obstacle to constructing a QFT circuit is that numerous elementary gates are required. Among the elementary gates, T gates dominate the cost of fault-tolerant implementation. Currently, the smallest-known T-count required to construct an n-qubit QFT circuit approximated to error $O(\varepsilon)$ is $\sim 8n\log_2(n/\varepsilon)$. Moreover, the depth of T gates (T-depth) in the approximate QFT circuit is $\sim 2n\log_2(n/\varepsilon)$. This approximate QFT circuit was constructed using Toffoli gates and quantum adders. In this study, we present a new n-qubit QFT circuit approximated to error $O(\varepsilon)$. Our approximate QFT circuit shows a T-count of $\sim 4n\log_2(n/\varepsilon)$ and a T-depth of $\sim n\log_2(n/\varepsilon)$. Toffoli gates, which account for half of the T-count in the approximate QFT circuit reported in the previous study, are unnecessary in our construction. Quantum adders, which dominate the leading order term of T-depth in our approximate QFT circuit, are arranged in parallel to reduce T-depth.

1. Introduction

The quantum Fourier transform (QFT) is perhaps the most versatile component of quantum algorithms. It is a key component of many quantum algorithms, such as Shor's factoring algorithm [1], quantum amplitude estimation algorithm [2], Harrow–Hassidim–Lloyd algorithm for linear systems of equations [3], and algorithms for security purposes [4–6]. Therefore, reducing the cost of implementing QFT would be crucial for the efficiency of many quantum algorithms.

Most quantum algorithms are implemented using quantum circuits. To implement large-scale quantum algorithms, it is necessary to construct quantum circuits using universal and fault-tolerant gates because quantum information is considerably fragile. Clifford + T gates are used such gates for various quantum error correction codes. Among these gates, Clifford gates can be constructed fault-tolerantly utilizing transversal operations. However, to implement the T gate fault-tolerantly, transversal construction cannot be used [7, 8], and relatively expensive methods, such as state distillation [9], are required. Therefore, when constructing quantum circuits, the number of T gates (T-count) should be optimized to execute quantum algorithms efficiently.

Until now, the smallest-known value of the T-count in an n-qubit QFT circuit approximated to error $O(\varepsilon)$ is $\sim 8n log(n/\varepsilon)$, as reported in Ref. [10]. Among the $\sim 8n log(n/\varepsilon)$ T gates, approximately half is used to construct relative phase Toffoli gates, and the other half is used to construct quantum adders. The approximate QFT circuit construction process in Ref. [10] can be briefly described as follows:

(1) Remove all controlled–R_k gates with angles smaller than a certain threshold value in the standard QFT circuit illustrated in Ref. [11] (see Figure 1), where $k \in \{2,3,4, \dots, n\}$.

The threshold value is chosen to satisfy the error-bound constraint of QFT implementation.

$$\text{Controlled} - R_k \text{ gate} = \begin{pmatrix} 1 & 0 & 0 & 0 \\ 0 & 1 & 0 & 0 \\ 0 & 0 & 1 & 0 \\ 0 & 0 & 0 & e^{\frac{i\pi}{2^{k-1}}} \end{pmatrix} \tag{1}$$

(2) Construct R_z gate layers using relative phase Toffoli gates and measurements. Each R_z gate layer forms a phase gradient transformation (PGT) circuit. A brief description of PGT can be found in Section 2B.

$$R_z(\theta) = e^{-i\theta/2} \begin{pmatrix} 1 & 0 \\ 0 & e^{i\theta} \end{pmatrix} \tag{2}$$

(3) Replace R_z gate layers with quantum adders reported in Ref. [12].
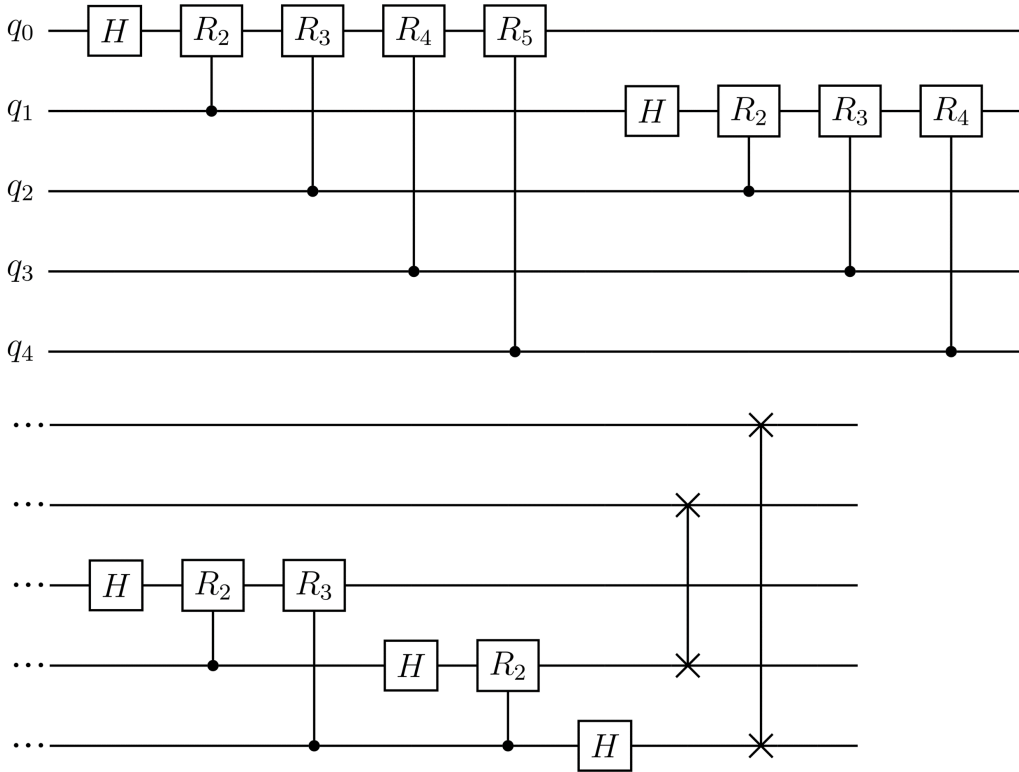

FIG. 1. Standard 5-qubit QFT circuit illustrated in Ref. [11].

3

In this study, we present a new n-qubit QFT circuit approximated to error $O(\varepsilon)$. Our approximate QFT circuit requires $\sim 4n\log(n/\varepsilon)$ T gates. The brief process of constructing our approximate QFT circuit is as follows:

(1) Construct the R_z gate layers. Each R_z gate layer forms an inverse PGT circuit.

(2) Remove all R_z gates with angles smaller than a certain threshold value in the QFT circuit. The threshold value was chosen to satisfy the error-bound constraint of the QFT implementation.

(3) Replace R_z gate layers with quantum adders reported in Ref. [12].

The approximate QFT circuit reported in Ref. [10] uses Toffoli gates (more precisely, relative phase Toffoli gates and measurements) to construct the R_z gate layers. However, the R_z gate layers in our approximate QFT circuit are constructed without Toffoli gates. This reduces the T-count in the approximate QFT circuit. Compared with the approximate QFT circuit in Ref. [10], our approximate QFT circuit also has the advantage of a lower depth of T gates (T-depth). The approximate QFT circuit reported in Ref. [10] shows a T-depth of $\sim 2n\log(n/\varepsilon)$, whereas our approximate QFT circuit shows a T-depth of $\sim n\log(n/\varepsilon)$. This T-depth reduction is a consequence of parallelizations of R_z gate layers in our approximate QFT circuit construction.

Our paper is organized as follows. Section 2 provides the study background, focusing on QFT and PGT using quantum addition [13]. In Section 3, we construct our approximate QFT circuit, thereby presenting the T-count and T-depth in our approximate QFT circuit and conducting an error analysis. In Section 4, we summarize our paper and discuss the implications of our results.

4

2. Background

A. Quantum Fourier transform

The n-qubit QFT is defined as Eq. (3), where $|j\rangle$ is a computational basis state.

$$QFT|j\rangle = \frac{1}{\sqrt{2^n}} \sum_{k=0}^{2^n-1} e^{\frac{2\pi ijk}{2^n}} |k\rangle \qquad (3)$$

The standard n-qubit QFT circuit (Figure 1) comprises n Hadamard (H) gates, $n(n-1)/2$ controlled–R_k gates, and $[n/2]$ SWAP gates, where $k \in \{2,3,4 \dots n\}$ [11]. A SWAP gate is synthesized using three controlled–not (CNOT) gates. Therefore, all components of the standard QFT circuit except controlled–R_k gates can be synthesized using Clifford gates. In previous studies, several methods have been proposed to synthesize controlled–R_k gates [14–16]. In all these methods, the complete synthesis of a controlled–R_k gate requires R_z gates. In this study, we used the method proposed in Ref. [14] to synthesize controlled–R_k gates (Figure 2).
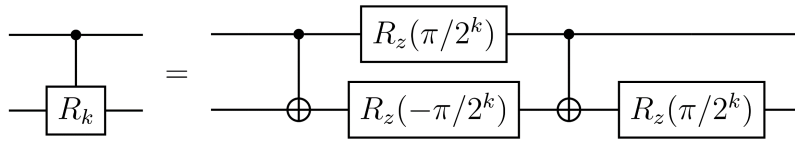

FIG. 2. Controlled–R_k gate decomposition in Ref. [14].

B. Phase gradient transformation

The PGT on a b-qubit system and its inverse are defined as Eq. (4) and (5), where $|k\rangle$ is a computational basis state.

$$PGT_b|k\rangle = e^{2\pi i k/2^b}|k\rangle \tag{4}$$

$$PGT_b^{-1}|k\rangle = e^{-2\pi i k/2^b}|k\rangle \tag{5}$$

In this study, we used inverse PGT. The remaining part of this section describes how to implement inverse PGT in a quantum circuit.

Inverse PGT can be executed on a b-qubit system using two methods. The first method uses a R_z gate layer, where each R_z gate in the layer has an angle of $-\pi/2^k$; here k is an integer from 0 to $b-1$. The circuit of the R_z gate layer is shown in Figure 3.
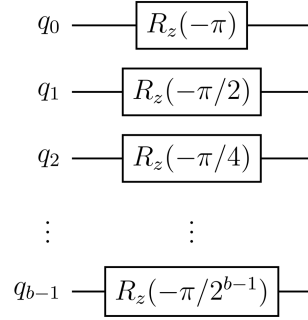

FIG. 3. Implementation of b-qubit inverse PGT using R_z gates.

The second method to implement inverse PGT on a b-qubit system involves using quantum addition modulo 2^b [13]. For this method, a b-qubit state $|\psi_b\rangle$ described by Eq. (6) must be prepared. The state $|\psi_b\rangle$ is prepared by applying b H gates and the R_z gate layer (Figure 3) with inverse angles to the state $|0\rangle^{\otimes b}$.

$$|\psi_b\rangle = \frac{1}{\sqrt{2^b}} \sum_{l=0}^{2^b-1} e^{\frac{2\pi i l}{2^b}} |l\rangle. \tag{6}$$

Next, we prove that the b-qubit inverse PGT can be implemented by adding the state $|\psi_b\rangle$ to

the state to which we want to apply inverse PGT. This proof uses the cyclic property of modulo addition and exponential function and is as follows:

$$
\begin{aligned}
ADD|k\rangle|\psi_b\rangle &= \frac{1}{\sqrt{2^b}} \sum_{l=0}^{2^b-1} e^{\frac{2\pi i l}{2^b}} |k\rangle|(k+l) mod\ 2^b\rangle \\
&= \frac{1}{\sqrt{2^b}} \sum_{l=0}^{2^b-1} e^{-\frac{2\pi i k}{2^b}} e^{\frac{2\pi i(k+l)}{2^b}} |k\rangle|(k+l) mod\ 2^b\rangle \\
&= e^{-\frac{2\pi i k}{2^b}} |k\rangle \frac{1}{\sqrt{2^b}} \sum_{l=0}^{2^b-1} e^{\frac{2\pi i(k+l)}{2^b}} |(k+l) mod\ 2^b\rangle \\
&= e^{-\frac{2\pi i k}{2^b}} |k\rangle \frac{1}{\sqrt{2^b}} \sum_{l'=0}^{2^b-1} e^{\frac{2\pi i l'}{2^b}} |l'\rangle \\
&= e^{-\frac{2\pi i k}{2^b}} |k\rangle|\psi_b\rangle
\end{aligned}
\tag{7}
$$

Note that there are two features of the method that use quantum addition to implement inverse PGT. The first feature is that the state $|\psi_b\rangle$ is preserved after inverse PGT implementation, i.e., the state $|\psi_b\rangle$ is reusable. The second is that if we have the state $|\psi_b\rangle$ and want to implement the inverse PGT on a b'-qubit system via quantum addition, where b' is smaller than b, the state $|\psi_{b'}\rangle$ does not have to be prepared separately because the state of partial qubits in the state $|\psi_b\rangle$ is $|\psi_{b'}\rangle$. This can be easily verified by considering the preparation of the states $|\psi_b\rangle$ and $|\psi_{b'}\rangle$ using H and R_z gates.

3. Results

A. Quantum Fourier transform circuit construction

In this section, we construct an n-qubit QFT circuit approximated to error $O(\varepsilon)$. The error analysis is presented in Section 3C. We use the circuit identities of Figures 2 and 4 in the

circuit construction process. The circuit identity of Figure 2 is from Ref. [14], and the circuit identities of Figures 4(a) and 4(b) are newly introduced in this study. The circuit identity of Figure 4(b) is a generalization of Theorem 4.1 reported in Ref. [17]. The circuit identities of Figure 4 can be proven easily by verifying how each computational basis state evolves through the circuits.
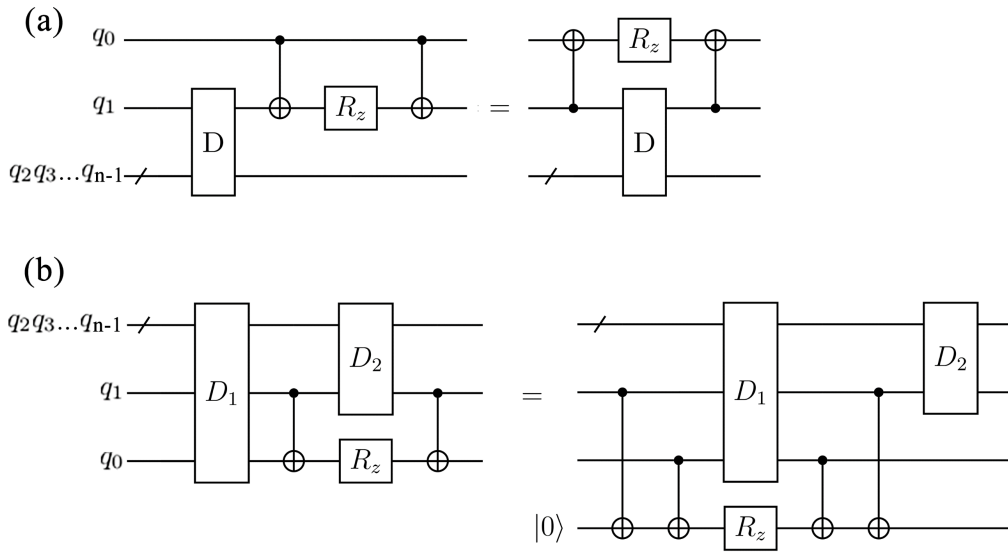

FIG. 4. Circuit identities. (a) A circuit identity that is used to create the R_z gate layers in our QFT circuit without using Toffoli gates. In the figure, D represents a circuit with a diagonal matrix representation. (b) A circuit identity that is used to parallelize R_z gate layers in our QFT circuit. In the figure, D_1 and D_2 represent circuits with diagonal matrix representation.

Our approximate QFT circuit construction process is as follows:

(1) Move the even-numbered H gates to the left in the standard QFT circuit as far as possible. Next, divide the QFT circuit into subcircuits following the illustration in Figure 5. Subsequently, we show subcircuit decomposition by considering the circuit of Figure 6(a) as an example.
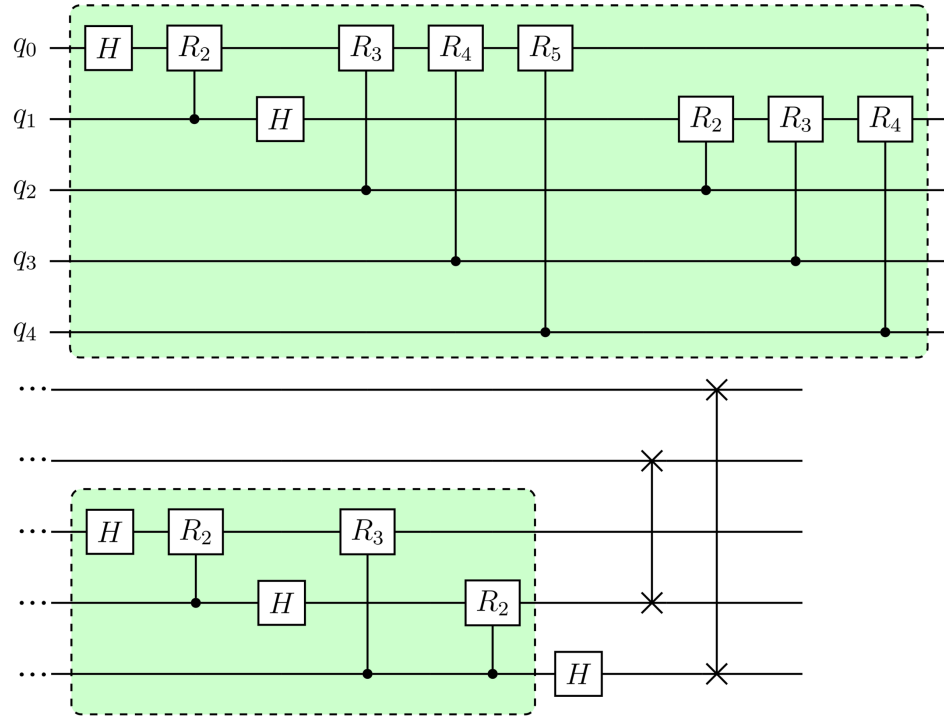
FIG. 5. A 5-qubit QFT circuit with moved H gates. Note that the even-numbered H gates of Figure 1 are moved to the left of the circuit as far as possible. The QFT circuit is divided into subcircuits in each green box. Figure 6 shows the decomposition of the subcircuits in each green box.

(2) Transform the subcircuit demonstrated in Figure 6(a) using the following process: Apply the circuit identity of Figure 2 to the circuit of Figure 6(a) and combine some R_z gates. Note that circuits with diagonal matrix representation commute. Next, apply the circuit identity of Figure 4(a). Then, the circuit of Figure 6(a) transforms into the circuit of Figure 6(b). Note that R_z gate layers are constructed without Toffoli gates. Apply the circuit identity of Figure 4(b) to the circuit of Figure 6(b), which further transforms the circuit of Figure 6(b) into the circuit of Figure 6(c). Note that two R_z gate layers are set in parallel.
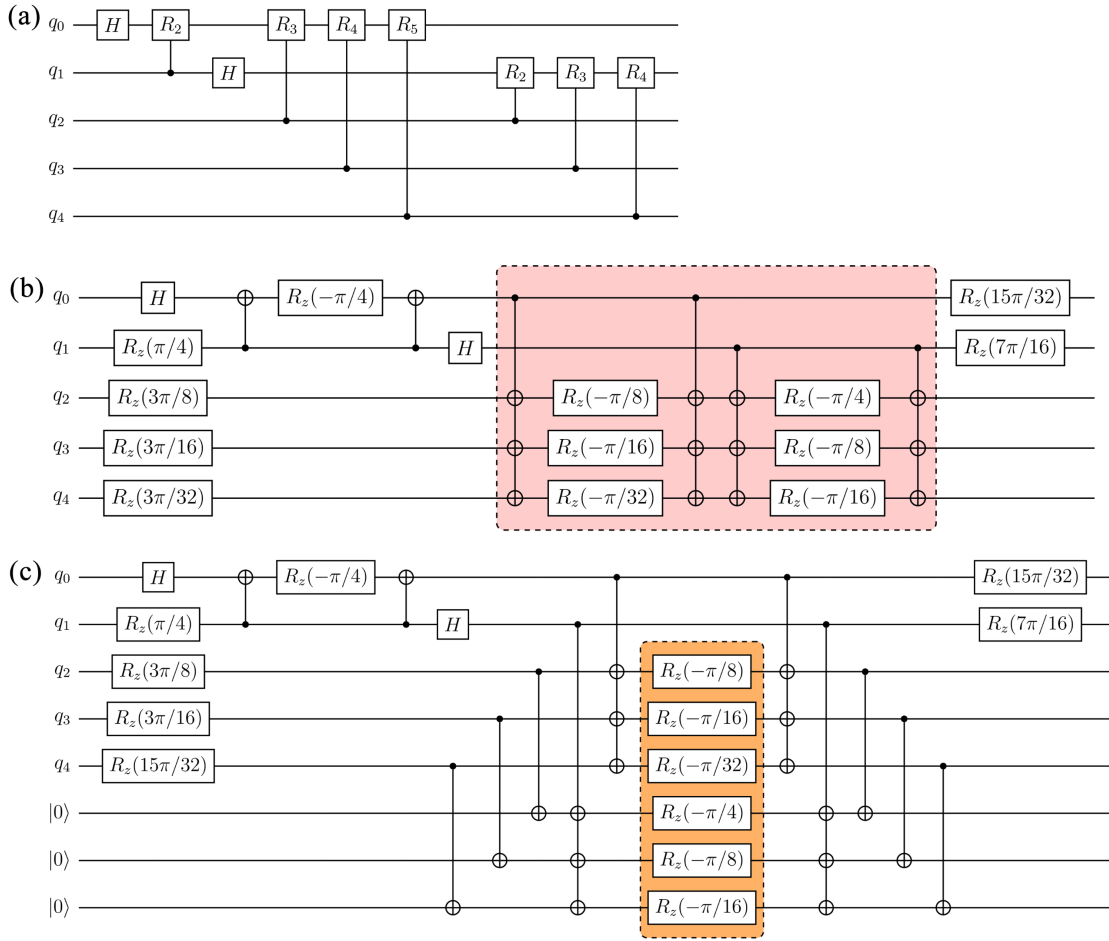
FIG. 6. Transformation of QFT subcircuits. (a) A subcircuit of the QFT circuit in Figure 5. (b) A circuit that performs the same operation as the circuit in Figure 6(a). Note that the R_z gate layers in the red box are constructed without Toffoli gates. (c) A circuit which performs the same operation as the circuit in Figure 6(a) and 6(b). Note that the two R_z gate layers in the red box in Figure 6(b) are combined to a single layer in the orange box in Figure 6(c) using ancilla qubits that are initially in the state $|0\rangle$.

(3) Combine the transformed subcircuits, such as the circuit of Figure 6(c), to construct a QFT circuit. Note that each R_z gate in the first and last R_z gate layers have an angle $(2^{k-1}-1)\pi/2^k$, where k is a positive integer.

(4) Divide each R_z gate in the first and last R_z gate layers into an S gate and an
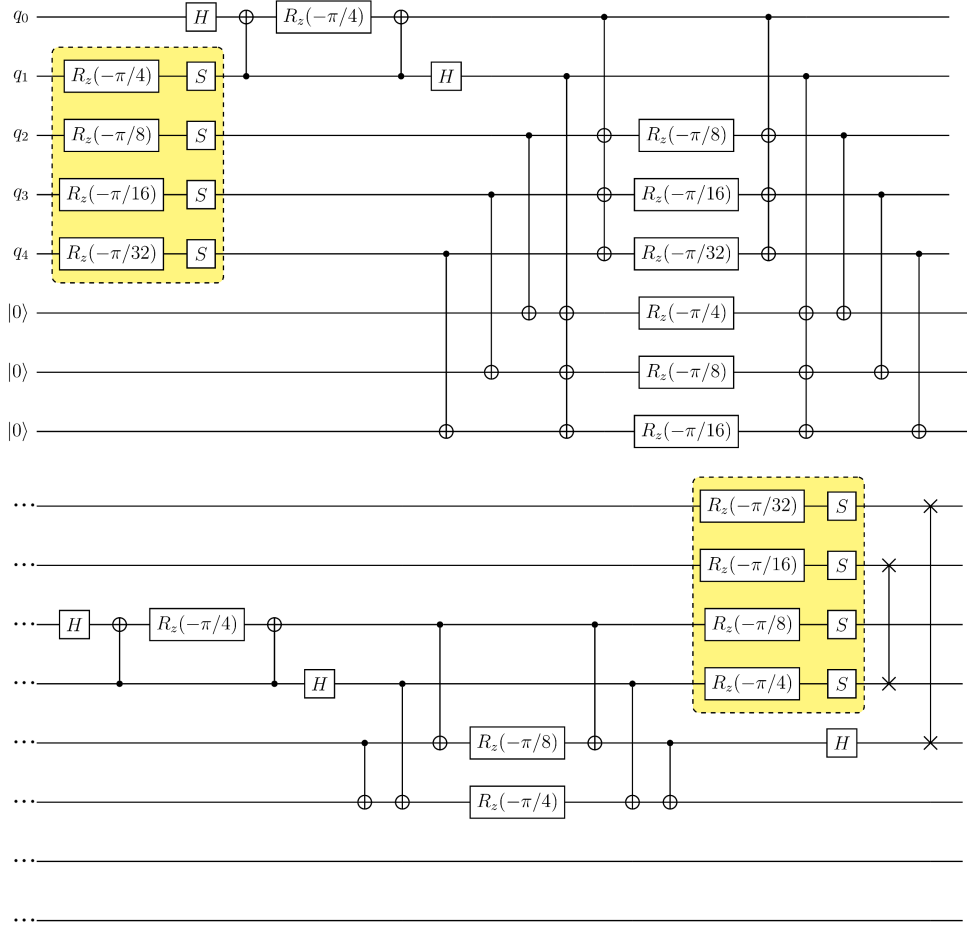
$R_z(-\pi/2^k)$ gate (see Figure 7).

FIG. 7. Decomposition of the 5-qubit QFT circuit. Note that in each yellow box, we divided each R_z gate into an S gate and an R_z gate.

Next, we proceed with approximation and replace the R_z gate layers with quantum adders.

(5) Approximation: Remove all R_z gates whose angles have absolute values that are smaller than $\pi/2^b$. We choose b as $\log_2(n/\varepsilon)$. Section 3C describes the reason we chose this value for b. For the convenience of description, we assume b to be a positive integer in the remainder of this paper.

11

(6) Insert $R_z(-\pi)$, $R_z(-\pi/2)$, and $R_z(-\pi/4)$ gates into the approximate QFT circuit to transform each R_z gate layer into an inverse PGT circuit, and add $R_z(\pi)$, $R_z(\pi/2)$, and $R_z(\pi/4)$ gates to nullify the effect of this insertion. This process increases the T-count by $\lceil n/2 \rceil$. After following the abovementioned process, the approximate QFT circuit has the circuit form shown in Figure 8.
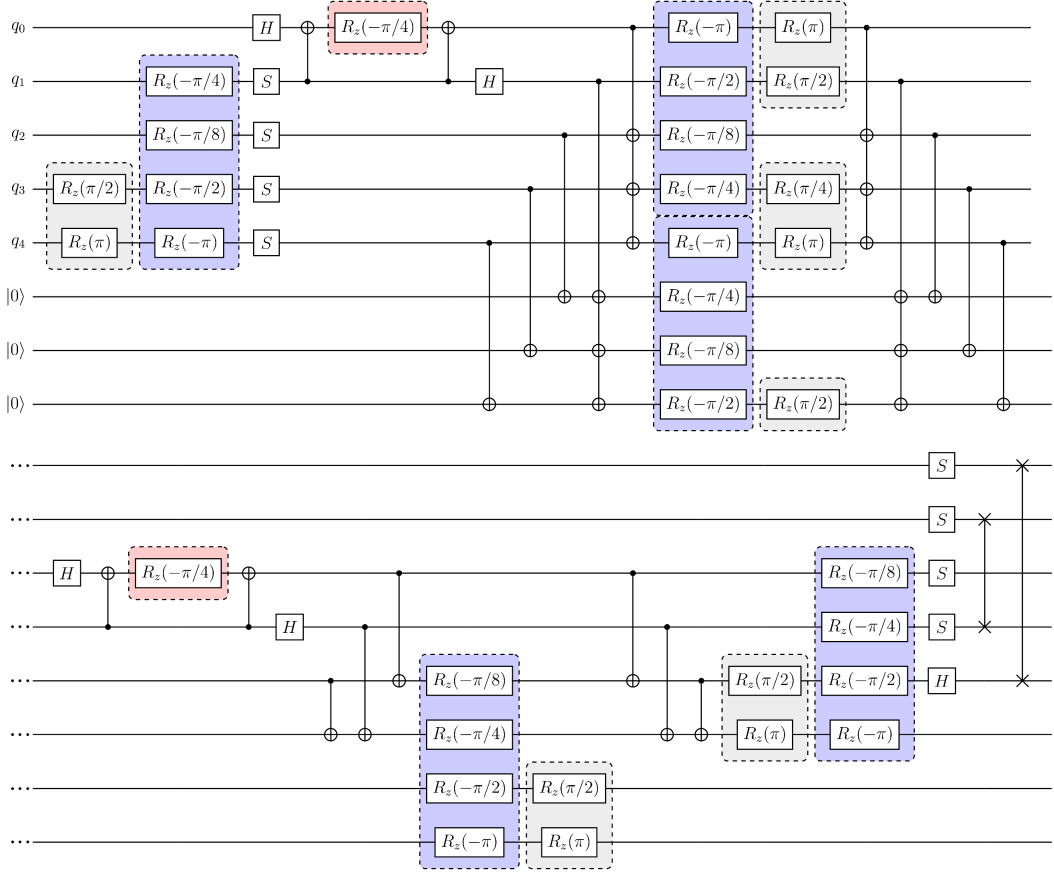

FIG. 8. Decomposition of the 5-qubit approximate QFT circuit. We removed all R_z gates whose angles have absolute values that are $< \pi/8$. The R_z gate layer in each blue box performs 4-qubit PGT and can be replaced with a quantum adder. The R_z gates in the gray boxes are added to nullify the effect of the R_z gates which were added in blue boxes to make the R_z gate layers perform inverse PGTs. The $R_z(-\pi/4)$ gates in the pink boxes are not related to PGTs.

(7) Replace R_z gate layers in the approximate QFT circuit with the $(b+1)$ qubit adders

that are constructed using the method reported in Ref. [12]. Note that the two $|\psi_{b+1}\rangle$s must be prepared to implement two quantum additions parallelly. Preparing two $|\psi_{b+1}\rangle$s requires $2(b+1)$ R_z gates. We synthesize each R_z gate approximately with an error of $\varepsilon/2b$ using the method reported in Ref. [18].

B. T-count and T-depth in the proposed quantum Fourier transform circuit

This section presents the required T-count and T-depth in our approximate QFT circuit. The T gates in our approximate QFT circuit is divided into four parts:

(1) T gates that are required to construct quantum adders

(2) T gates that are required for R_z gate synthesis to prepare two $|\psi_{b+1}\rangle$s

(3) $n/2 + O(1)$ T gates (See the gray boxes in Figure 8) that are used to nullify the effect of $R_z(-\pi/4)$ gates; here the $R_z(-\pi/4)$ gates are used to make the R_z gate layers perform inverse PGTs.

(4) $n/2 + O(1)$ T gates that are not related to PGTs (See the pink boxes in Figure 8)

First, we present the T-count required for quantum adders. To build a b-qubit quantum adder as reported in Ref. [12], we require $4(b-1)$ T gates. In our approximate QFT circuit construction, we need $(n-b+3)$ $(b+1)$-qubit adders and one each from $b, b-1, b-2, \ldots, 3$-qubit adders. Therefore, the required T-count for quantum adders is $4b(n-b+3) + 2(b+1)(b-2)$.

Second, we present the T-count required to prepare two $|\psi_{b+1}\rangle$s. To prepare a $|\psi_{b+1}\rangle$, $(b+1)$ R_z gates are required. Among these R_z gates, $R_z(\pi)$, $R_z(\pi/2)$, and $R_z(\pi/4)$ gates correspond to Z, S, and T gates, respectively. Therefore, we need to synthesize the

remaining $2(b-2)$ R_z gates using Clifford + T gates to prepare two $|\psi_{b+1}\rangle$s. Here, we used the method reported in Ref. [18] to synthesize R_z gates. When applying the method reported in Ref. [18], the T-count required to synthesize an R_z gate approximated to error ε' is $1.15 \log_2(1/\varepsilon') + O(1)$. Because we synthesized each R_z gate approximated to error $\varepsilon/2b$, the T-count value to prepare two $|\psi_{b+1}\rangle$s is $2.3(b-2)\log_2(2b/\varepsilon) + O(b)$.

Overall, our n-qubit QFT circuit approximated to error $O(\varepsilon)$ requires $4b(n-b+3) + 2(b+1)(b-2) + 2.3(b-2)\log_2(2b/\varepsilon) + n + O(b)$ T gates, where b is $\log_2(n/\varepsilon)$. Therefore, the leading-order term of the T-count value in our n-qubit approximate QFT circuit is $4n\log_2(n/\varepsilon)$.

Compared with the approximate QFT circuit in Ref. [10], our approximate QFT circuit also has advantages in terms of T-depth. The leading-order term of T-depth in the n-qubit QFT circuit approximated to error $O(\varepsilon)$ in Ref. [10] is from the T gates in quantum adders. The b-qubit quantum adder in Ref. [12] has a T-depth of $2(b-1)$, and the approximate QFT circuit in Ref. [10] requires roughly n b-qubit quantum adders. Therefore, the T-depth of the n-qubit approximate QFT circuit in Ref. [10] is $\sim 2n\log_2(n/\varepsilon)$. Whereas the leading-order term of the T-depth of our n-qubit approximate QFT circuit is $n\log_2(n/\varepsilon)$. This is because we pair the inverse PGTs (except the first and last ones; see Figure 8) and implement two quantum addition in parallel. The details of the T-depth of our approximate QFT circuit are as follows.

The T-depth in our approximate QFT circuit is also divided into four parts. The T-depth required for quantum adders is $b(n-b+1) + 2b + (b+1)(b-2)/2 + O(1)$ because we execute two quantum additions simultaneously. The T-depth required to prepare two $|\psi_{b+1}\rangle$s is $1.15\log_2(2b/\varepsilon) + O(1)$ because each R_z gate synthesis can be implemented in parallel. The T-depth of the remainder parts is $n + O(1)$. Therefore, our n-qubit QFT circuit

approximated to error $O(\varepsilon)$ requires an overall T-depth of $b(n - b + 1) + 2b + (b + 1)(b - 2)/2 + 1.15 \log_2(2b/\varepsilon) + n + O(1)$, where b is $\log_2(n/\varepsilon)$.

C. Error analysis

The error between quantum circuits U and V is defined as the spectral norm of $(U - V)$ [8]. This section demonstrates that our approximate QFT circuit has an error of $O(\varepsilon)$ compared to QFT circuit. The approximation error in our approximate QFT circuit construction is originated from two factors:

(1) The error resulting from the removal of R_z gates whose angles have absolute values that are $< \pi/2^b$.

(2) The error of gate synthesis for preparing two $|\psi_{b+1}\rangle$s.

First, we present the error of removing R_z gates. If one $R_z(-\pi/2^p)$ gate is removed from a circuit, the error is $\|1 - e^{i\pi/2^p}\|$, which is $< \pi/2^p$. Here, $\|\cdot\|$ denotes the l_2 norm. In our approximate QFT circuit construction process, the maximum error caused by removing R_z gates from an R_z gate layer that performs PGT is $\sum_{p=b+1}^{n} \pi/2^p$, which is $< \pi/2^b$. We removed R_z gates from $(n - b + 3)$ R_z gate layers. Therefore, the error caused by the removal of R_z gates from QFT circuit has an upper bound of $\pi(n - b + 3)/2^b = \pi(n - b + 3)/n$. If $b > 3$, then the error is $< \pi\varepsilon$.

Next, we present the error resulting from the synthesis of R_z gates to prepare two $|\psi_{b+1}\rangle$s. Since we synthesized $2(b - 2)$ R_z gates, each of which is approximated to error $\varepsilon/2b$, the error caused by the synthesis of R_z gates has an upper bound of $\varepsilon(b - 2)/b$, which is $< \varepsilon$. Therefore, the total error, which includes errors from removing R_z gates and gate

15

synthesis to prepare two $|\psi_{b+1}\rangle$s is $< \varepsilon(\pi + 1)$, i.e., $O(\varepsilon)$.

4. Discussion

Overall, we present a new n-qubit QFT circuit approximated to error $O(\varepsilon)$. The leading-order term of the T-count in our approximate QFT circuit is $4nlog_2(n/\varepsilon)$, which is asymptotically half of the smallest-known T-count ($\sim 8nlog_2(n/\varepsilon)$) of the approximate QFT circuit in Ref. [10]. Moreover, in terms of T-depth, our approximate QFT circuit is superior to the approximate QFT circuit reported in Ref. [10]. The T-depth of the approximate QFT circuit in Ref. [10] is $\sim 2nlog_2(n/\varepsilon)$, whereas that of our approximate QFT circuit is $\sim nlog_2(n/\varepsilon)$.

QFT is a fundamental tool for many quantum algorithms, particularly quantum algorithms that are exponentially faster than classical algorithms. However, for practical uses, most of those algorithms are too large for implementation on noisy devices. Therefore, fault-tolerant implementation of QFT should eventually be realized to take complete advantage of quantum computing. By reducing the cost of the fault-tolerant implementation of QFT, our study may accelerate the realization of fault-tolerant quantum computing.

Acknowledgments

expressed are those of the authors, and do not reflect the official policy or position of IBM or the IBM Quantum team.

Author declarations

Conflict of interest

The authors have no conflict of interest.

Author contributions

B. P. Formal analysis (lead); Validation (lead); Writing (equal). **D. A.** Fundamental idea (lead); Supervision (lead); Writing (equal).

Data availability

The data that support the findings of this study are available from the corresponding author upon reasonable request.

References

1   P. W. Shor, *SIAM Rev.* **41**, 303 (1999).

2   G. Brassard, P. Hoyer, M. Mosca, and A. Tapp, *Contemp. Math.* **305**, 53 (2002).

3   A. W. Harrow, A. Hassidim, and S. Lloyd *Phys. Rev. Lett.* **103**, 150502 (2009).

4   Y. G. Yang, X. Jia, S. J. Sun, and Q. X. Pan, *Inf. Sci.* **277**, 445 (2014).

5   W. Yang, L. Huang, R. Shi, and L. He, *Quantum Inf. Process.* **12**, 2465 (2013).

6   W.-W. Zhang, F. Gao, B. Liu, Q.-Y. Wen, and H. Chen, *Quantum Inf. Process.* **12**, 793 (2013).

7   E. T. Campbell, B. M. Terhal, and C. Vuillot *Nature* **549**, 172 (2017).

8   B. Eastin and E. Knill, *Phys. Rev. Lett.* **102**, 110502 (2009).

9   S. Bravyi and A. Kitaev, *Phys. Rev. A* **71**, 022316 (2005).

10   Y. Nam, Y. Su, and D. Maslov, *npj Quantum Inform.* **6**, 1 (2020).

11   M. A. Nielsen and I. L. Chuang, *Quantum Computation and Quantum Information: 10th Anniversary Edition* (Cambridge University Press, 2011).

12   C. Gidney, *Quantum* 2, 74 (2018).

13   A. Y. Kitaev, A. Shen, and M. N. Vyalyi, *Classical and quantum computation* (American Mathematical Society, Providence, 2002).

14   A. Barenco, C. H. Bennett, R. Cleve, D. P. DiVincenzo, N. Margolus, P. Shor, T. Sleator, J. A. Smolin, and H. Weinfurter, *Phys. Rev. A* **52**, 3457 (1995).

15   M. Amy, D. Maslov, M. Mosca, and M. Roetteler, *IEEE Trans. Comput. Aided Design Integr. Circuits Syst.* **32**, 818 (2013).

16   T. Kim and B. S. Choi, *Sci Rep* **8**, 1 (2018).

17   P. Selinger, *Phys. Rev. A* **87**, 042302 (2013).

18   A. Bocharov, M. Roetteler, and K. M. Svore, *Phys. Rev. Lett.* **114**, 080502 (2015).